Capacitive scanning dilatometry and frequency-dependent thermal expansion of polymer films

C. Bauer, R. Böhmer,* S. Moreno-Flores,† R. Richert,‡ and H. Sillescu
Institut für Physikalische Chemie, Johannes Gutenberg-Universität, 55099 Mainz, Germany

D. Neher
Institut für Physik, Universität Potsdam, 14415 Potsdam, Germany
(Received 9 August 1999)

The dilatometric properties of polymer films near and above their glass-transition temperatures were explored using capacitive high-frequency detection in temperature ramping as well as in harmonic temperature cycling experiments. The broad applicability of capacitive scanning dilatometry is demonstrated by the investigation of macromolecular systems of vastly different polarity such as polystyrene, polybutadiene, and polyvinylacetate. From temperature cycling experiments the real and imaginary parts of the frequency-dependent thermal-expansion coefficient are determined in the sub-Hz regime.

PACS number(s): 61.41.+e, 64.70.Pf

I. INTRODUCTION

Entropy and volume are among the most basic thermodynamic quantities characterizing amorphous polymers [1]. It has long been recognized that in the glass-transformation range these properties depend on the experimental conditions, with important parameters being the thermal sample history and the time scale used for measurement. Entropy, probably the parameter most often determined in the laboratory, is not measured directly but rather its temperature derivative, which is related to the heat capacity, is measured. In order to cover a large time or frequency range, a number of different calorimetric methods are in use. Among them are temperature ramping techniques such as differential scanning calorimetry (DSC) [2] and temperature cycling methods [3], as well as high-precision enthalpy relaxation measurements based on the application of temperature jumps [4].

The measurement of time-dependent thermal expansion coefficients via the observation of volume changes in the glass-transformation range is also not new [5]. Mercury dilatometry has often been used to investigate the volume variations of organic specimens following a temperature jump [1,6,7]. X-ray scattering and other methods have also been employed for this purpose [8]. Capacitive dilatometry, another standard technique in this area, has mostly been used to study equilibrium properties [9], but occasionally was also performed in temperature ramping mode [10]. In capacitance dilatometry, an air gap between the (electrically conducting) sample surface and a nearby counterelectrode usually represents the capacitive element. In order to achieve good sensitivity, the air gap typically is very narrow and hence special precautions are necessary to ensure sufficient mechanical stability.

In this article we report on the development of a simple yet reliable capacitive method with which to determine thermal expansion properties of thin films of glass-forming material. The basic idea is to use the specimen itself as the dielectric material [11] in the capacitor rather than an air gap. However, with the sample sandwiched between the electrodes, our method is sensitive not only to the thermal but also to the dielectric characteristics of the specimen. Using suitable experimental conditions, useful information on thermal properties can nevertheless be obtained. One way to achieve this would of course be to restrict our attention to nonpolar or only weakly polar polymers, such as polystyrene (PS). In order to show that the method of capacitive scanning dilatometry (CSD) is not restricted to this class of materials, in addition to PS we have studied two other amorphous polymers, viz. 1,4-polybutadiene (PB) and polyvinylacetate (PVAc). As we will show, the sensitivity of our method not only to thermal but also to dielectric material characteristics lends itself to a particularly simple means to detect the liquid fragility.

Capacitive methods are usually not sensitive to the volume expansion (which is often detected using mercury dilatometers) but rather to the linear thermal expansion. If one of the geometrical parameters (either the gap or the area) of the capacitor containing the specimen under study is fixed, then a clamped thermal expansion coefficient, α_C, is measured. In the thin-film geometries chosen for this work we explore both the constant gap and the constant area conditions, yielding α_{CG} and α_{CA}, respectively. We will show that our dilatometer can be operated not only in a temperature ramping but also in a temperature cycling mode. This makes it possible to determine the complex frequency-dependent thermal expansion, $\alpha_C^*(\omega,T)$. Although below we are able to derive thermal-expansion coefficients from our experimental results which agree well with literature data, the emphasis of the current work is mostly on mapping out the dynamic aspects of the dilatometric properties of amorphous polymers.

II. THEORETICAL CONSIDERATIONS

A. Nonequilibrium thermal expansion

Let us suppose that a temperature jump ΔT (applied at time $t=0$) changes a characteristic dimension of our speci-

*Electronic address: bohmer@aak.chemie.uni-mainz.de
†Permanent address: Departamento di Química Física, Universidad Complutense, 28040 Madrid, Spain.
‡Permanent address: Department of Chemistry and Biochemistry, Arizona State University, Tempe, AZ 85287-1604.

men from l_0 to l. Then from the definition of the coefficient of linear thermal expansion $\alpha_p = l^{-1}(\partial l/\partial T)_p$ (taken at constant pressure p) the normalized length change, $\lambda \equiv (l - l_0)/l_0$, for sufficiently long times after the temperature step is $\lambda = \alpha_p \Delta T$. In general, the response to ΔT will not be entirely instantaneous. Denoting the short-time (or glassy) thermal expansion coefficient as $\alpha_{p,g}$ and the long-time (or liquidlike) one as $\alpha_{p,l}$, one can write

$$\alpha_p(t) = \lambda(t)/\Delta T = \alpha_{p,g} + (\alpha_{p,l} - \alpha_{p,g})[1 - \Phi(t)]. \quad (1)$$

In order to see what the associated correlation function $\Phi(t)$ (normalized to decay from 1 to 0) is, it is instructive to note that the thermodynamic quantities, heat capacity, $C_p = T(\partial S/\partial T)_p$, and compressibility, $\kappa_T = V^{-1}(\partial V/\partial p)_T$ can be related to fluctuations in the extensive variables entropy S and volume V, respectively. Likewise, the coefficient of thermal expansion can be expressed in the static case as the cross fluctuation between the variables S and V via $\alpha_p = \langle \Delta S \Delta V \rangle / (3 k_B T V)$ [12]. This equation includes fluctuating quantities such as $\Delta S(t) = S(t) - \overline{S}$, with the bar denoting a time average. With the use of an appropriately formulated fluctuation-dissipation theorem [13], the above relation can be generalized to read in the frequency domain [14]

$$\alpha_p(\omega) = (3 k_B T V)^{-1} \int \left(-\frac{d}{dt} \langle \Delta S(0) \Delta V(t) \rangle \right) e^{i\omega t} dt. \quad (2)$$

Thus the desired correlation function is given by $\Phi(t) = -d\langle \Delta S(0) \Delta V(t) \rangle / dt$. The sine and cosine transforms of $\Phi(t)$ define a complex susceptibility $\alpha_p^*(\omega) = \alpha_p'(\omega) + i\alpha_p''(\omega)$. If the temperature is varied sinusoidally around a constant mean with frequency ω, then α' and α'' simply denote the in-phase and out-of-phase components of the associated normalized length variations. From experience with other complex susceptibilities determined near the glass transition, it may be anticipated that in general $\alpha^*(\omega)$ will not be governed by a single time scale. Corresponding findings are often accounted for by the introduction of phenomenological distribution functions [15]. Then, in the time domain the ensemble-averaged correlation functions decay in a nonexponential fashion.

Temperature ramping experiments are more complicated to deal with, since in this case nonlinearities and hysteresis effects arise almost inevitably. From the number of approaches developed in the past to treat this situation, those based on the introduction of a so-called fictive temperature, T_f, have been quite successful in terms of rationalizing experimental data. T_f is a parameter which is meant to describe the instantaneous structural state of a glass former. It differs from the thermodynamic temperature as soon as the sample is brought into a nonequilibrium state [16]. Using the conventional definition of fictive temperature one way write

$$\alpha_p(T) = \alpha_{p,g} + (\alpha_{p,l} - \alpha_{p,g}) dT_f/dT, \quad (3)$$

In analogy to the treatment for the heat capacity T_f can be modeled in a number of different ways [3]. Below we will use what is sometimes referred to as the Narayanaswamy-Moynihan approach. It is based on the numerical solution of the equation

$$T_{f,n} = T_0 + \sum_{j=1}^{n} \Delta T_j \left\{ 1 - \exp\left[-\left(\sum_{k=j}^{n} \frac{\Delta T_k}{q_k \tau_k} \right)^{\beta} \right] \right\}. \quad (4)$$

with the initial temperature $T_0 \equiv T_{f,0}$. In order to perform explicit calculations, the ramping rate $q_k \equiv \Delta T_k / \Delta t_k$ has to be defined for each time step Δt_k. Furthermore, the dependence of the relaxation time τ on T and T_f needs to be specified in Eq. (4). Assuming the familiar Adam-Gibbs equation to be applicable, one can write $\tau_k = \tau_0 \exp\{B/[T_k(1 - T_2/T_{f,k-1})]\}$ [17]. Thus in order to calculate $T_f(T)$ there are four fitting parameters: the attempt frequency $1/\tau_0$, the effective barrier B, and the divergence temperature T_2, as well as the Kohlrausch exponent β, the latter describing the nonexponentiality of the structural relaxation.

B. Geometrically restricted expansion

If an isotropic body is subjected to a temperature jump ΔT, then the relative change $\lambda_x = \Delta l_x / l_x$ of its length l_x along the x direction, as well as those along the other directions, can be derived from the appropriate combination of Hooke's and Poisson's relations [18] and yields

$$\lambda_x = E^{-1}[\sigma_x - \nu(\sigma_y + \sigma_z)] + \alpha_p \Delta T, \quad (5a)$$

$$\lambda_y = E^{-1}[\sigma_y - \nu(\sigma_x + \sigma_z)] + \alpha_p \Delta T, \quad (5b)$$

$$\lambda_z = E^{-1}[\sigma_z - \nu(\sigma_x + \sigma_y)] + \alpha_p \Delta T. \quad (5c)$$

Thus, in order to specify the relation between the extensions λ_i and the stresses σ_i of an isotropic body, two independent elastic constants are needed. In Eq. (5) these are the isothermal extensional (Young's) modulus, E, and the isothermal Poisson ratio, ν, i.e., the ratio of longitudinal expansion to transverse contraction. In order to account for various geometrically restricting conditions, relevant in the present context, one needs to specify which are of the expansions and/or stresses zero. Under conditions of constant area A (taken to lie in the x-y plane) one has $\lambda_x = \lambda_y = \sigma_z = 0$. Evaluating Eq. (5), the normalized expansion along the z direction (this is what we call the clamped longitudinal expansion coefficient α_{CA}) is derived to be

$$\alpha_{CA} = \lambda_z / \Delta T = \alpha_p (1 + \nu)/(1 - \nu). \quad (6)$$

One commonly has $0 \leqslant \nu \leqslant 0.5$ [19]. This implies that $\alpha_{CA} \geqslant \alpha_p$ with the equality arising for $\nu = 0$ (meaning that longitudinal compression would lead to no lateral stresses). In the liquid state, where the bulk modulus K is much larger than the shear modulus G, the Poisson ratio is $\nu = (3K/G - 2)/(6K/G + 2) \approx 0.5$ and consequently $\alpha_{CA} = 3\alpha_p/(1 + 4G/K) \approx 3\alpha_p$. This means that the expansion of the sample, which would normally occur in the lateral dimensions, but which now is impeded by the geometrical restrictions, leads to an enhancement of expansivity in the longitudinal direction. The length change along the z axis then is of course maximum if the body is incompressible.

Taking the electrode again to lie in the x-y plane, for conditions of a constant gap d one has $\sigma_x=\sigma_y=\lambda_z=0$. This leads to the lateral thermal expansion coefficient $\alpha_{CG}=\lambda_x/\Delta T=\lambda_y/\Delta T$. This clamped coefficient is

$$\alpha_{CG}=(1+\nu)\alpha_p . \tag{7}$$

The enhancement factor $1+\nu=3/[2+2G/(3K)]$ expected for a given Poisson ratio is smaller compared to the one appearing in Eq. (6), since unrestricted expansion is now possible along two directions. Furthermore, this also implies that variations of ν have less impact on the clamped thermal expansion α_{CG} than on α_{CA}. Variations of ν are expected to show up near the glass transition, since here bulk and shear modulus depend upon frequency and temperature. It is a fortunate circumstance, however, that while the enhancement factors appearing in Eqs. (6) and (7) typically [20] change by less than 30%, the linear thermal expansion coefficients change by typically 300%. Our considerations show that for a more quantitative determination of α_p from thin-film investigations, information about Poisson's ratio is required. Furthermore, we should emphasize that the treatment presented in this section starts from the consideration of an isotropic body. However, particularly for the constant-gap geometry a distribution of lateral mechanical stresses cannot be ruled out with certainty. A quantitative evaluation of such effects is beyond the scope of the present paper.

C. Capacitive detection

If a dielectric material expands along a direction normal to the capacitor electrodes rigidly attached to its surfaces, i.e., if the capacitor gap increases, it is immediately obvious that its capacitance $C=\varepsilon_0\varepsilon_\infty A/d(\equiv\varepsilon_\infty C_0=\varepsilon_0\varepsilon_\infty l_x l_y/l_z)$ decreases. Here ε_0 denotes the permittivity of free space. There are, however, more subtle effects. Due to the variation of density the dielectric constant ε_∞ itself changes even if the molecular polarizability α_{mol} is constant. The changes in the high-frequency dielectric constant can be derived from the Lorenz-Lorentz equation [21] $(\varepsilon_\infty-1)/(\varepsilon_\infty+2)=\alpha_{mol}N/(3\varepsilon_0 Al_z)$, where $\rho=N/(Al_z)$ is the density, i.e., the number N of polarizable units per volume. Then the derivative with respect to any of the variables, ζ, appearing on the right-hand side of the Lorenz-Lorentz equation is $d\varepsilon_\infty/d\zeta=\pm\zeta^{-1}K(\varepsilon_\infty)$, with $K(\varepsilon_\infty)=(\varepsilon_\infty-1)(\varepsilon_\infty+2)/3$ and the plus sign for ζ appearing in the numerator and the minus sign otherwise. In order to obtain the total variation in the capacitance, we may write $dC=(\partial C/\partial C_0)_\varepsilon dC_0+(\partial C/\partial\varepsilon_\infty)_{C_0}d\varepsilon_\infty$ or

$$\frac{dC}{dT}=\varepsilon_\infty\frac{dC_0}{dT}+C_0\frac{d\varepsilon_\infty}{dT}. \tag{8}$$

First, Eq. (8) will be evaluated under constant area conditions. With $(dC_0/dT)_A=(dC_0/dl_z)_A(dl_z/dT)_A=-C_0\alpha_{CA}$ and $(d\varepsilon_\infty/dT)_A=(d\varepsilon_\infty/dl_z)_A(dl_z/dT)_A=-K(\varepsilon_\infty)\alpha_{CA}$ one has

$$\alpha_{CA}=\frac{-1}{[\varepsilon_\infty+K(\varepsilon_\infty)]C_0}\left(\frac{dC}{dT}\right)_A . \tag{9}$$

Under constant-gap conditions only the density ρ changes but the geometric capacitance, C_0, is invariant, i.e., $dC_0/dT=0$. The change in density is then simply given by $\Delta\rho/\rho=-(\lambda_x+\lambda_y)$. Using the expression for α_{CG} appearing just above Eq. (7) one has $\Delta\rho/\Delta T=-2\rho\alpha_{CG}$. Combining this result with $(d\varepsilon_\infty/dT)_{l_z}=(d\varepsilon_\infty/d\rho)_{l_z}(d\rho/dT)_{l_z}$ one finally finds that

$$\sigma_{CG}=\frac{-1}{2K(\varepsilon_\infty)C_0}\left(\frac{dC}{dT}\right)_{l_z} . \tag{10}$$

Thus in both cases the clamped thermal-expansion coefficients are given by the derivative of the logarithmic capacitance, $d(\ln C)/dT$, times a correction factor which for small ε_∞ depends relatively weakly on the geometry. Taking $\varepsilon_\infty=2.5$, say, one has $\varepsilon_\infty+K(\varepsilon_\infty)=4.75$ and $2K(\varepsilon_\infty)=4.5$.

III. EXPERIMENT DETAILS

Three different polymers were used for this study. Thin films of atactic polystyrene (molecular weight $M_w=119\,000$ g/mol) of variable thickness were produced either by spin coating or by drop casting polymer solutions and subsequent drying at elevated temperatures. The thickness of these films was determined using a profilometric device (Alpha-Step 2000 from Tencor Instruments) and was found to lie in the 1–10-μm range with a surface roughness of typically $\pm5\%$. The spin-coated films were contacted by 100-nm-thick Al electrodes evaporated onto the polymer surface with the lower electrode previously deposited onto a thin glass plate. The cast films were supported by a bottom electrode made of brass. Here the upper electrode consisted of an In foil topped with a brass plate. The foil was used to ensure tight contact between the sample surface and brass electrode. The active electrode area of the different capacitor arrangements ranged from 30 to 80 mm^2. No significant differences between films prepared by spin coating or drop casting were found. For PVAc ($M_w=14\,500$ g/mol) only cast films were used. The PB sample material [55% 1,4-*trans*, 35% 1,4-*cis*, 10% 1,2-(vinyl); $M_w=12\,400$ g/mol] used in the present investigation was described in detail previously [22]. For the investigation of this relatively fluid sample we have used a cell made of sapphire and invar steel which has been optimized for a temperature-invariant geometry [22,23]. In this construction the electrode is mainly defined by the invar steel part, such that constant-gap conditions (about 90 μm) may be assumed as a good approximation [24]. The thickness of all samples was large enough so that bulk behavior can be expected. Confinement-induced effects typically show up for samples thinner than about 0.3 μm [11,25]. Since the emphasis of the present study is on mapping out the frequency and time dependence of the thermal expansion and not so much on obtaining highly accurate absolute values, we have not used guard-ring electrodes. Nevertheless, we were able to reproduce numerical values of the thermal-expansion coefficient as reported in the literature within experimental uncertainty (see Sec. V below). This shows that no corrections taking into account the small expansion coefficients of the electrode materials are necessary, as may be rationalized by noting that they are considerably smaller than those of the polymers under study.

The capacitor assemblies with calibrated Pt sensors attached in close proximity to the thin polymer films were thermostatted using a commercial system from Novocontrol. This system allowed us to apply a dry stream of nitrogen gas with an arbitrary temperature program. Using the standard regulation capabilities of our system, we could achieve maximum cooling or heating rates $0.1\,\mathrm{K/min} < |q| < 4.5\,\mathrm{K/min}$. Smaller rates were reached by repeated stepping of the temperature by typically 0.15 K and subsequent stabilization. The maximum cycling frequency was 10 mHz.

In order to obtain a well defined temperature across the polymer film, it is necessary that its surface be in good contact with a substrate which on the one hand exhibits no lateral temperature gradients and on the other hand has a heat capacity much larger than the polymer film. Both conditions are met in our experiments. Because the sample cell materials are good thermal conductors relative to the environmental N_2 gas, we expect that the temperature changes are applied uniformly over the electrode area and that the sensor temperatures match those at the electrode surface. In order to ensure that no longitudinal gradients show up, the thermal ''skin depth,'' l_t, is required to be much larger than the film thickness. With a thermal diffusion coefficient $D_{\mathrm{th}} = l_t^2/\tau$ of typically $10^{-3}\,\mathrm{cm}^2/\mathrm{s}$, the skin depth at our largest temperature modulation frequency $\omega = 1/\tau = 2\pi \times 10\,\mathrm{mHz}$ is more than 1 mm. Since the equivalent time scales involved in the ramping experiments are even longer (see below), longitudinal gradients are also not expected to be a problem. Nevertheless, due to the large thermal mass of the sapphire/invar cell, it may be expected that the largest usable modulation frequency is lower than for the thin-film assemblies.

For the measurement of the complex dielectric constant we used a Solartron SI-1260 gain/phase analyzer equipped with a Mestec DM-1360 transimpedance amplifier. The dilatometric results reported in this article correspond to time scales of seconds or longer. In order to minimize interference of the dilatometric with the dielectric relaxation processes, it is mandatory to measure the capacitance on much shorter time scales, or, equivalently, at larger detection frequencies f_D. Unless otherwise specified, we use $f_D \approx 550\,\mathrm{kHz}$ for PS and PB. For PVAc, which exhibits a much larger dielectric strength than the other two polymers, it turned out to be necessary to employ a larger detection frequency (we use $f_D = 10\,\mathrm{MHz}$).

IV. RESULTS AND ANALYSES

A. Capacitive scanning dilatometry

In order to ensure that our dilatometric measurements in the glass-transformation range are not affected by the dielectric relaxation processes, we have first determined the variation of the capacitance C as a function of frequency. Results for PS taken at a cooling rate of -0.08 K/min are presented in Fig. 1. The high-frequency capacitances show a clear break in slope near the conventional glass-transition temperature. The relatively steep increase in $C(T)$ observed upon cooling from high temperatures is a consequence of the increase in the density of the polymeric melt. Below T_g the thermal-expansion coefficient drops and consequently $C(T)$ increases in a less pronounced fashion. For low detection frequencies the upturn in $C(T)$ observable upon increasing

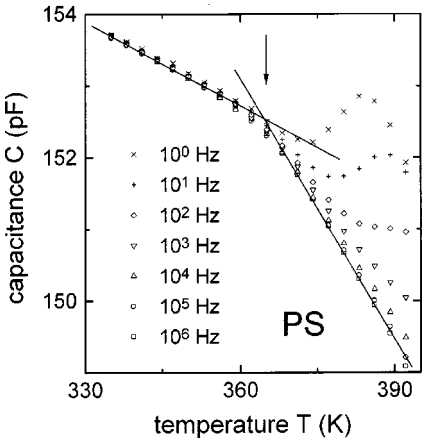

FIG. 1. Frequency-dependent capacitance C of PS as measured upon cooling with $q = -0.08\,\mathrm{K/min}$. The solid lines are drawn to represent the linear dependences of C in the glassy and liquid regimes. From their intersection the glass-transition temperature may be read.

the temperature marks the presence of dielectric relaxations. Figure 1 thus gives a visual impression of the temperature range in which the results for a given detection frequency f_D are unaffected by dipolar reorientation processes. It is clear that due to the ever-increasing speedup of the dielectric response, at temperatures larger than those shown in Fig. 1 the capacitance signal will also start to reflect the dielectric relaxation behavior even for the highest frequencies employed for the present study.

The temperature at which the change of slope occurs (cf. Fig. 1) can be shifted considerably by employing different cooling rates q. This is documented for the polymers PS and PVAc in Fig. 2 for a variation of q over a range of about 2 decades. The data are represented in normalized form as

$$\delta(T) \equiv [C(T) - C(T_0)]/C(T_0), \tag{11}$$

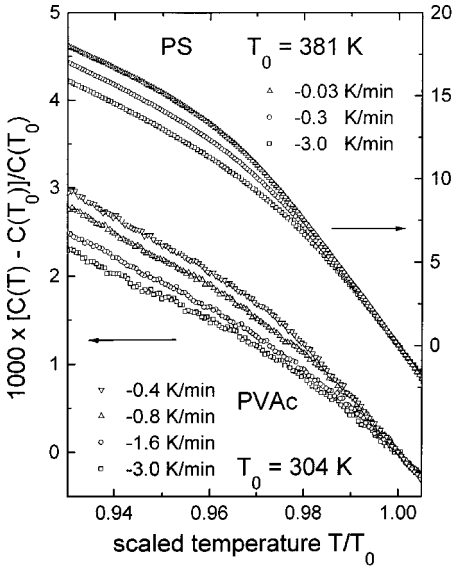

FIG. 2. Normalized capacitance of PVAc (left-hand scale) and PS (right-hand scale) as measured for various cooling rates in constant-area geometry. The data for PVAc were collected at 10 MHz, those for PS at 460 kHz. The normalization temperatures T_0 are indicated in the figure.

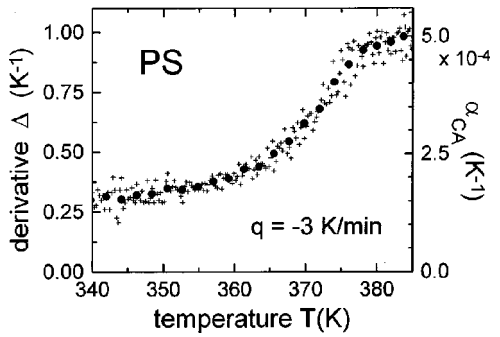

FIG. 3. Temperature derivative $\Delta(T) \equiv -1000 \times d\delta(T)/dT$ of $\delta(T) = [C(T) - C(T_0)]/C(T_0)$ with $T_0 = 381$ K. The input data for PS were taken from Fig. 2. We show both the raw data (crosses) and results (dots) obtained by averaging over nine measurements.

vs T, with T_0 being a reference temperature. From run to run $C(T_0)$ changed by less than 0.11% (PS) and 0.07% (PVAc) for the cast films and less than 0.015% for the spin-coated films, demonstrating the good stability of our specimens. Under constant-gap conditions of a reproducibility 0.03% was achieved. It is evident from Fig. 2 that, despite quite similar thermal-expansion behavior, the relative capacitance variation of PS is much larger than that of PVAc. This is due to the fact that for the latter polymer the detection frequency of 10 MHz is still not large enough to avoid interference with dielectric properties. In other words, dipolar relaxation processes lead to an increase in the capacity onto which the thermal expansion behavior is superimposed. Nevertheless, the general thermal features, such as the rate-dependent break in slope and the increase in capacitance, hence decrease in fictive temperature upon slow cooling, are still observed.

Figure 3 is a plot of the derivative,

$$\Delta(T) \equiv -1000 \frac{d[\delta(T)]}{dT}, \tag{12}$$

of the $q = -3$ K/min data for PS as shown in Fig. 2. The derivative $\Delta(T)$, which may be considered an effective expansion coefficient, is somewhat noisy; therefore, we have usually employed an averaging procedure. Typically, the mean value from 7 to 11 adjacent data points is shown. The averaged results are also presented in Fig. 3 for comparison. The ordinate axis on the right-hand side of Fig. 3 shows the clamped thermal-expansion coefficient α_{CA} that was computed from Eq. (9) and $\varepsilon_\infty = 2.5$. It is seen that α_{CA} changes by a factor of about 3 through the glass-transformation range.

In Fig. 4(a) we present data taken for PVAc upon cooling at 0.4 K/min and subsequent reheating at the same rate. The two curves differ in a systematic fashion. While the cooling curve shows a smooth change of slope, in the heating data this effect is much more pronounced. This is due to the fact that upon reheating, a retarded response shows up. The asymmetry between heating and cooling runs is related to the nonlinearity of the structural response under nonequilibrium conditions. It leads to a related asymmetry in temperature stepping experiments [4], and is associated with the overshoot phenomenon [cf. Fig. 4(b)]. The upturn in $C(T)$ evident for $T > 310$ K and also the curved behavior showing up

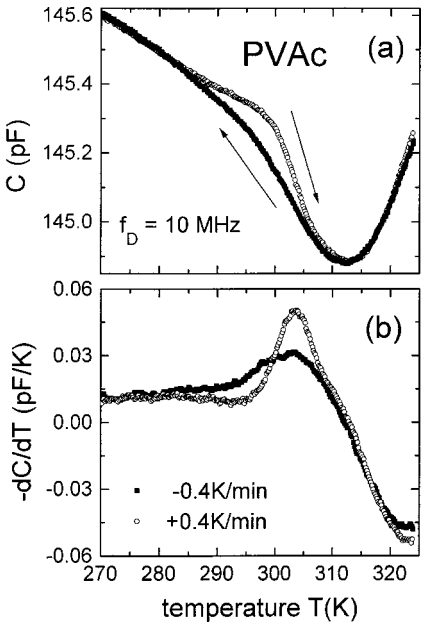

FIG. 4. (a) Capacitance of a spin-coated PVAc film as measured upon ramping the temperature with a rate $|q| = 0.4$ K/min. The sample was first cooled down to 270 K and then reheated immediately. The arrows indicate the direction of temperature change. (b) Smoothed temperature derivative of the capacitance data shown in the upper frame.

at somewhat lower temperatures is due to the onset of the thawing of dielectric degrees of freedom.

In Fig. 4(b) we show the temperature derivative, $-dC(T)/dT$, of the data presented in Fig. 4(a). Below about 305 K the derivative signal exhibits pronounced hysteresis effects. Here, in the glass-transformation range, the cooling curve indicates a smooth variation while the heating run yields a well defined overshoot. This latter feature is well known also from DSC investigations and allows for a convenient determination of an onset glass-transition temperature [2]. Above 305 K the derivative data are obviously not dominated by dilatometric properties. They are nevertheless shown here to document the relatively small thermal lag between cooling and heating runs. This observation confirms that for the thin films our temperature sensor is in good thermal contact with the polymeric specimen.

In Fig. 5 we present a similar set of data for PB as measured using the constant-gap geometry. Due to the use of a rigid electrode assembly, this geometry makes possible a determination of the dielectric properties up to temperatures far above T_g. Thus in Fig. 5(a) not only the break in slope due to the dilatometric glass transition is seen. Also, similarly to the case of PVAc, an upturn in the capacitance shows up at higher temperatures, and then, more importantly, a local maximum is observed in $C(T)$. Somewhat below the temperature at which this maximum is located, we find a dielectric loss peak signaling that the time scale characterizing the dipolar degrees of freedom is about 1 μs. In Fig. 5(c) the derivative signal is depicted for several detection frequencies. Above approximately 185 K dielectric and dilatometric properties are no longer well separated.

The results presented in this section demonstrate that our

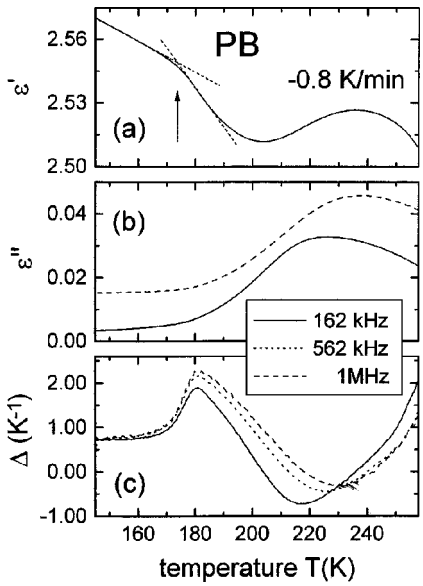

FIG. 5. (a) Dielectric constant of PB as measured upon cooling in constant-gap geometry. The capacitance of the empty cell was 32.1 pF. The inflection point near 220 K indicates the slowing down of the dipolar degrees of freedom on a time scale of $\tau_{1/2}=(2\pi \times 162\ \mathrm{kHz})^{-1}\approx 1\ \mu\mathrm{s}$. The break in slope near 175 K (marked by an arrow) signals the dilatometric glass transition. (b) Dielectric loss as detected for two different frequencies f_D. The loss measured at 1 MHz has been shifted upward for clarity. (c) Derivative signals $\Delta(T)$ with $C(T_0)$ replaced here by the geometric capacitance. This plot demonstrates that, even for the highest f_D used here, no plateau region is reached above the step showing up near T_g.

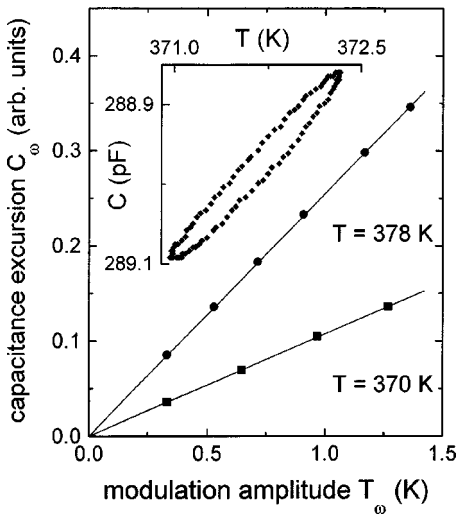

FIG. 6. Capacitance oscillation amplitudes recorded for PS upon cycling the temperature at 4 mHz using various modulation amplitudes T_ω. The straight lines indicate linearity up to a surprisingly large T_ω. The inset shows a Lissajous pattern obtained for $\omega/2\pi = 1$ mHz. Note the inverted labeling of the ordinate axis of the inset.

method, CSD, is a useful tool with which to study the dilatometric glass transition of polymeric materials. Quantitative analyses of the dynamic aspects, which we will discuss in more detail below (Sec. IV), are complicated by the same nonlinearities that also affect the outcome of other ramping experiments, such as DSC. In the field of heat-capacity spectroscopy it has proven useful to apply temperature cycling techniques in order to circumvent these problems [3,26]. In the following, we report on efforts to carry out related experiments aimed at determining the frequency-dependent, complex thermal-expansion coefficient $\alpha^*(\omega)$.

B. Thermal expansion spectroscopy

For the measurement of $\alpha^*(\omega)$ we have modulated the temperature of our specimens sinusoidally and recorded the capacitance $C(t)$ and the temperature $T(t)$, usually for more than 10 cycles. By waiting a sufficiently large number of periods prior to the data acquisition, we have ensured that our samples are structurally stabilized, i.e., that they are not affected by physical aging. In particular, we have discarded the data from the first few cycles of each run in order to eliminate transient effects. In the inset of Fig. 6 we show a typical set of raw data plotted as $C(t)$ vs $T(t)$. This representation yields an ellipse that may be described by $T(t) = \overline{T} + T_\omega e^{-i\omega t}$ and $C(t) = \overline{C} + C_\omega e^{-(i\omega t+\theta)}$. In order to determine the amplitudes T_ω and C_ω, as well as the phase lag, θ, we have performed a harmonic analysis [27]. In a subsequent step, we have varied the temperature modulation amplitude and recorded the magnitude of the capacitance excursions in order to determine if our experiment operates in the linear-response regime. The result of this procedure is shown in Fig. 6 for two different temperatures. It is seen that $C_\omega \propto T_\omega$, at least for $T_\omega \leqslant 1.4$ K, which is much larger than the oscillation amplitude used in the remainder of the present work [28]. The slope C_ω/T_ω, via Eq. (9), is directly proportional to the magnitude of the coefficient of thermal expansion. From this information and the knowledge of the phase lag, θ, the imaginary part of α^* can be determined [29].

The clamped thermal-expansion coefficient determined experimentally for PS is presented in Fig. 7 for a temperature cycling frequency of $\omega/2\pi = 4$ mHz. At first glance, the real part, α'_{CA}, looks like the cooling curve shown in Fig. 3.

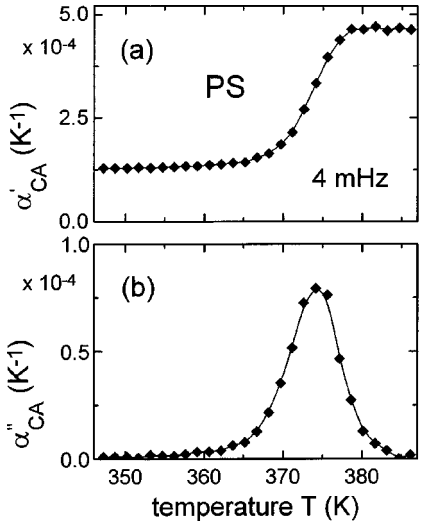

FIG. 7. In-phase and out-of-phase components of the clamped thermal-expansion coefficient, $\alpha_{\mathrm{CA}}(T)$, for PS recorded at a temperature-modulation frequency of 4 mHz. Lines are drawn to guide the eye.

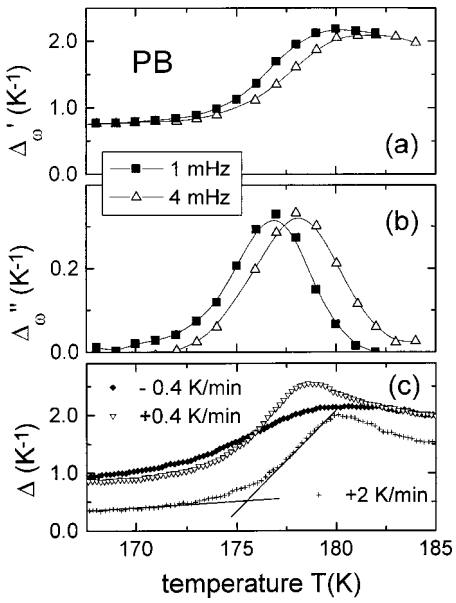

FIG. 8. Effective thermal expansion of PB. Frames (a) and (b) show the in-phase and out-of-phase components of $\Delta_\omega^*(T)$ recorded at two different temperature modulation frequencies. The lowest frame represents data taken upon ramping the temperature between $T>230\,\mathrm{K}$ and $T=150\,\mathrm{K}$. The data measured upon heating with 2 K/min were shifted vertically for clarity. From the intersection of the straight lines the onset T_g was determined. Lines are drawn to guide the eye.

However, it should be realized that, in contrast to the situation in the ramping experiments, the data shown in Fig. 7 were taken in metastable equilibrium. Near the temperature where $\alpha'_{\mathrm{CA}}(T)$ is steepest, the loss part $\alpha''_{\mathrm{CA}}(T)$ shows a well defined peak indicating that the dilatometric response time is of the order $\tau=\omega^{-1}\approx 40\,\mathrm{s}$. For PB we have carried out analogous measurements in constant-gap geometry with the experimental results obtained at two different temperature modulation frequencies shown in Fig. 8. The data are again represented in terms of the derivative quantity which in the case of the modulation experiment is complex, $\Delta_\omega^*\equiv\Delta'_\omega+i\Delta''_\omega$, and, in the temperature range shown in Fig. 8, it is proportional to α_{CG}. It is clearly seen that the position of the steps in $\Delta'_\omega(T)$ and of the peaks in $\Delta''_\omega(T)$ are frequency dependent. As we have seen in Fig. 5 for temperatures $T>185\,\mathrm{K}$, the dilatometric properties are no longer well separated from the dielectric effects for the detection frequency f_D used. Therefore, no data at higher temperatures are shown in Fig. 8.

In addition to the measurements presented in Fig. 8, we have performed a cycling experiment at $\omega/2\pi=10\,\mathrm{mHz}$. It turned out that the magnitude of α_{CG} was somewhat smaller than expected from the measurements taken at lower modulation frequencies (not shown). However, by multiplying the apparent expansion coefficients at 10 mHz by a factor of 1.3, a complete overlap of all data taken in the nondispersive temperature regime could be obtained. From this observation we conclude that in constant-gap geometry the thermal contact between sample and temperature sensor (provided by the invar electrodes) for the modulation frequency of 10 mHz is not as ideal as it is for the lower frequencies.

V. DISCUSSION

Our experimental results demonstrate that the simple CSD technique is a useful tool with which to investigate nonequilibrium dilatometric properties of polymer films. But of course it can also yield information on (quasi)static properties such as the coefficient of linear expansion in the liquid or the glassy states. From our ramping measurements on the spin-coated and drop-cast films as well as from the temperature cycling experiments on PS we find, using Eq. (6), that $\alpha_{p,g}=(7.0\pm 0.5)\times 10^{-5}\,\mathrm{K}^{-1}$ and $\alpha_{p,l}=(15.5\pm 1.0)\times 10^{-5}\,\mathrm{K}^{-1}$. Here we have utilized $\nu=0.33$ for the glassy state and $\nu=0.5$ for the liquid [30]. The fact that our $\alpha_{p,l}$ value is about 10% smaller than the published one may indicate that the assumption of a constant area is not perfectly met but is, rather, a good approximation only. It is highly plausible that in the liquid state the polymer film will not stick perfectly to the supporting substrate and hence be able to expand slightly in the lateral directions. This will lead to a slight decrease of the longitudinal expansion, as is experimentally observed. The good agreement of the limiting thermal-expansion coefficients with published values gives us confidence that the simple treatment presented in Sec. II provides a reasonably good description of the experimental situation. In particular, this statement implies that, at least for the case of PS, distributions of lateral stresses may be considered sufficiently small and the detection frequency employed here is large enough to justify the use of the Lorenz-Lorentz equation, which is valid only if the contributions from orientational polarizations play no role.

In order to describe ramping experiments quantitatively, we have employed the fictive temperature approach based upon Eqs. (3) and (4). This procedure has often been used before to analyze DSC data. Empirical parameters describing the calorimetric results of PS under a number of different ramping conditions have been reviewed in an article by Hodge [31]. From the parameters $\ln(\tau_0/\mathrm{s})=-63.5$, $B=7630\,\mathrm{K}$, $T_2=260\,\mathrm{K}$, and $\beta=0.54$ as given in that paper we have calculated the normalized thermal expansion $\alpha_N\equiv[\alpha_{\mathrm{CA}}(T)-\alpha_{\mathrm{CA},g}]/(\alpha_{\mathrm{CA},l}-\alpha_{\mathrm{CA},g})=dT_f/dT$ [cf. Eq. (3)] via Eq. (4) using $\Delta T=0.2\,\mathrm{K}$ between 393 and 328 K. In Fig. 9 we compare the results of the computations with our experimental data. It is seen that the agreement is very good. This indicates that the calorimetric and dilatometric results are closely related [32]. The relationship between the underlying thermodynamic quantities (C_p and α_p, but also κ_T), which may be expected on the basis of suitable thermomechanical models [33], will not be discussed here.

A note of caution regarding the parameters obtained from analyzing ramping data within the fictive temperature approach seems to be in order. It has been reported that these parameters may not be very well defined for a given material, since they can apparently depend on the ramping rates [34]. In particular, determination of the stretching exponent β (assumed to be constant in the calculations, but known to be temperature dependent for many materials) seems to be difficult in temperature-scanning investigations.

In order to compare the time scales from CSD directly with those from the modulation experiments, in Fig. 10 we have plotted characteristic temperatures for PB from both techniques. The characteristic temperatures we use are (i)

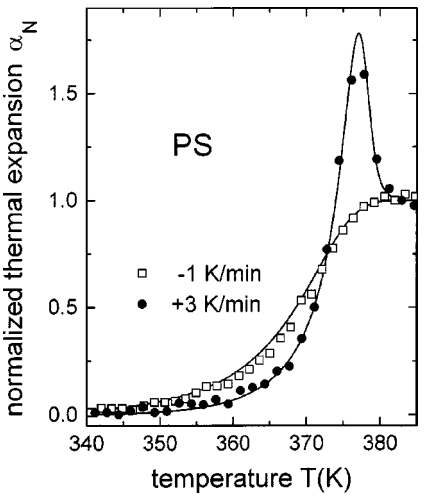

FIG. 9. Normalized thermal expansion $\alpha_N(T) \equiv [\alpha_{CG}(T) - \alpha_{CA,g}]/(\alpha_{CA,l} - \alpha_{CA,g})$ of PS. The experimental results were obtained by cooling to 328 K and immediate reheating. They are represented by the symbols. The solid lines refer to dT_f/dT with T_f computed according to Eq. (4) and the parameters given in Ref. [31].

$T_g(q)$ as determined from the break of slope of $C(T)$ [cf. Fig. 5(a)], (ii) the ramping-rate-dependent onset temperatures as shown in Fig. 8(c), as well as (iii) the peak temperatures from $\Delta''_\omega(T)$ [cf. Fig. 8(b)]. When plotting these temperatures versus the ramping rate [(i) and (ii)] or versus the modulation frequency (iii) it is seen that they are all compatible with a shift factor of $a_T = 1.9$ K/decade. The representation in Fig. 10 is chosen such that it facilitates a direct comparison of modulation frequencies and hence relaxation times with the cooling rates. One can see that $q = -10$ K/min (open circles, left-hand scale of Fig. 10), say, yields the same characteristic freezing temperature that

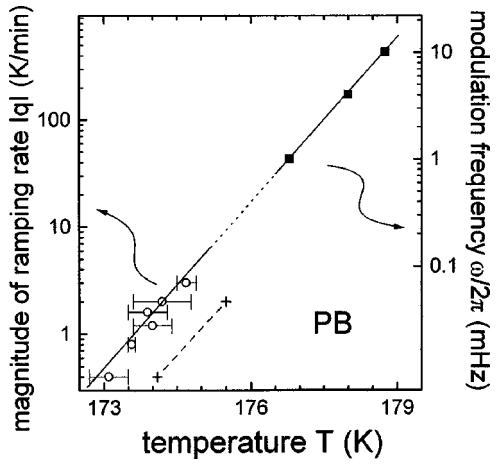

FIG. 10. Characteristic freezing (or glass-transition) temperatures of PB as obtained under various experimental conditions. The scale on the left-hand side corresponds to T_g determinations from the break of slope detected upon cooling [circles, cf. Fig. 5(a)] and from the onset observed during rate heating subsequent to cooling with -0.4 K/min [crosses, cf. Fig. 8(c)]. Data from the modulation experiments (full squares) obtained from the maxima of Δ''_ω correspond to the axis on the right-hand side. The lines represent a shift factor of $a_T = 1.9$ K/decade.

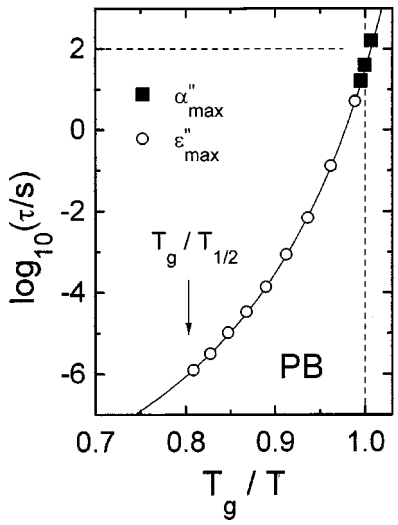

FIG. 11. Angell plot for PB incorporating relaxation times obtained from the maxima of the imaginary parts of the dilatometric and dielectric susceptibilities. The arrow indicates $T_{1/2}/T_g$ from which the fragility index $F_{1/2} = 2T_{1/2}/T_g - 1$ can immediately be determined. We find $F_{1/2} = 0.61$. The solid line is a fit using a Vogel-Fulcher expression.

would have been expected for a cycling frequency of $\omega/2\pi = 0.23$ mHz (right-hand scale of Fig. 10). Employing the relation $\omega\tau = 1$, one therefore concludes that the rate $q = -10$ K/min, say, corresponds to an average structural relaxation time τ of about 700 s. If, alternatively, T_g is determined from the onset construction (crosses in Fig. 10), rather than from the break in slope (circles), then a rate of 10 K/min corresponds to about $\tau = \omega^{-1} = 150$ s. This number is compatible with the familiar notion that the calorimetric glass-transition temperature is associated with a structural relaxation time of about 100 s [35].

Previous experience with supercooled melts shows that time scales derived from different experiments such as, e.g., calorimetric and viscoelastic spectroscopy often closely parallel one another. In Fig. 11 we have plotted relaxation times from dielectric and dilatometric measurements in a T_g-scaled or Angell plot. The steepness $m = d[\log_{10}(\tau/s)]/d(T_g/T)|_{T=Tg}$ of the relaxation time curve [36], commonly referred to as the fragility index, can then easily be determined from the data. The m index can be obtained from the data directly or, alternatively, from a phenomenological expression, such as the Vogel-Fulcher relation written as

$$\tau = \tau_0 \exp[DT_K/(T - T_K)]. \tag{13}$$

Here the divergence temperature is denoted T_K. With $\tau_0 = 10^{-14}$ s the fragility is related to the parameter D via $m = m_{min} + m_{min}^2 \ln 10/D$ and $m_{min} = 16$ [37]. Recently, an alternative definition of a fragility index $F_{1/2}$ has been suggested: $F_{1/2} \equiv 2T_g/T_{1/2} - 1$ [38]. This index depends on two reference temperatures only and thus is similar to the indices defined in Ref. [39]. In the above expression $T_{1/2}$ is the temperature at which the relaxation time $\tau_{1/2}$ is halfway between its value at T_g and $T \to \infty$, i.e., $\log_{10}(\tau_{1/2}/s) \equiv [\log_{10}(\tau_0) + \log_{10}(\tau_g)]/2 = -6$. If a particular form for $\tau(T)$, such as

the Vogel-Fulcher expression, is chosen, the two definitions of fragility are of course completely equivalent. They are related via [39]

$$m = m_{\min}\frac{1+F_{1/2}}{1-F_{1/2}} = m_{\min}\frac{T_g}{T_{1/2}-T_g}. \tag{14}$$

The right-hand side shows how m can be determined if in addition to T_g, $T_{1/2}$ is also known. And with these two reference points, T_K can simply be obtained from $T_g=(T_K+T_{1/2})/2$.

One of the advantages of the $F_{1/2}$ fragility is that it is particularly simple to determine. One only needs to carry out measurements that are sensitive to motions on time scales near $\tau_{1/2}$ as well as near τ_g. This determination should be particularly reliable if the corresponding temperatures can be gained in a single experiment. Such an experiment has recently been devised by Ito *et al.* [40]. These authors augmented their DSC setup with a dielectric sample heating unit operated at a frequency $\nu_{1/2}=1/(2\pi\tau_{1/2})$. One can alternatively use a dielectric experiment with a detection frequency near $\nu_{1/2}$ provided it is also sensitive to relaxation processes near T_g. This is of course just what some of the experiments described in this article are designed for.

In Fig. 11 we have plotted the relaxation times determined from the peak maxima of the out-of-phase parts of the dielectric and of the dilatometric responses. It is seen that the time constants from the two experiments nicely agree with one another. A similar observation was also made for PS (not shown) [41]. The time constants for PB can be described using the Vogel-Fulcher expression, Eq. (13), with $\log_{10}(\tau_0/\mathrm{s})=-11.2$, $B=380\,\mathrm{K}$, and $T_K=148\,\mathrm{K}$. The ratio $T_{1/2}/T_g$ can easily be read off from the plot and gives $F_{1/2}=0.61$. The fragility index thus estimated from Eq. (14), $m=66$, is similar to that observed for 1,4-*cis*-polyisoprene ($m=62$) [36]. These fragility indices are among the lowest reported for polymeric materials so far. It should be noted, however, that a direct determination of the slope of the relaxation time data near T_g gives a somewhat larger m index for PB. This is probably due to the fact that for temperatures $T \gg T_g$ the dielectric peak frequencies are affected not only by the structural relaxation, but also by the Johari-Goldstein β process [22].

Due to the rather limited frequency range available to the present temperature cycling technique we have not attempted to map out the explicit frequency dependence of the coefficients of thermal expansion. In order to obtain a rough estimate of the stretching of the dilatometric response, one can, however, use the normalized maximum out-of-phase component, $N=\alpha''/(\alpha_1'-\alpha_g')$. If only a single relaxation time is present, then $N=\frac{1}{2}$, otherwise N is smaller. With the functional form of the stretching of the response parametrized, e.g., via the familiar Kohlrausch function, $\Phi(t) \propto \exp[-(t/\tau)^\beta]$, the relation between N and the stretching parameter β can be computed numerically [42]. Assuming that the stretching here is of the Kohlrausch form, we find for PS that $N=0.24\pm0.01$ (cf. Fig. 7), hence $\beta=0.43\pm0.02$. For PB the same N is found from Fig. 8 and the stretching parameter obtained here is similar to that estimated from the dielectric loss peaks. A more detailed analysis of the data obtained for PS, including a comparison of time scales from dielectric and dilatometric measurements, will be published elsewhere [41].

VI. CONCLUSION

In this article we have presented a simple technique useful for characterizing the dilatometric response of polymeric films in their glass-transformation range. Our capacitive method works best for polymers with a weak to moderate dielectric relaxation strength. The experiment was operated in two different modes. In the ramping mode (capacitive scanning dilatometry), temperature derivative signals are obtained that look similar to those from differential scanning calorimetry. For CSD, cooling runs are very simple to perform for a wide range of ramping rates. This may be considered an advantage in comparison to the capabilities of many DSC setups. The second mode of operation involves a harmonic modulation of the sample temperature. Using this experiment, the in-phase and out-of-phase dilatometric responses can be mapped out. It should be noted that one of the advantages of the current technique is that it is also well suited to an investigation of films that are much thinner than the approximately micron-thick specimens used for the current study. Due to the increase in capacitance and the concomitant gain in sensitivity, reliable determinations of T_g down to a thickness of about 10 nm become possible [11].

ACKNOWLEDGMENTS

We thank T. Christensen, G. Diezemann, and N. B. Olsen for stimulating discussions.

[1] For early reviews, see, W. Kauzmann, Chem. Rev. **43**, 219 (1948); R. O. Davies and G. O. Jones, Adv. Phys. **2**, 370 (1953); A. J. Kovacs, Fortschr. Hochpolym.-Forsch. **3**, 394 (1963).

[2] An excellent review containing numerous references is I. M. Hodge, J. Non-Cryst. Solids **169**, 211 (1994).

[3] A good overview is given by the articles in Thermochim. Acta **304/305**, (1997).

[4] See, e.g., H. Fujimori, H. Fujita, and M. Oguni, Bull. Chem. Soc. Jpn. **68**, 447 (1995).

[5] See, e.g., E. Jenckel, Z. Elektrochem. **43**, 796 (1937)).

[6] R. Greiner and F. R. Schwarzl, Rheol. Acta **23**, 378 (1984).

[7] Inorganic glass-formers have also been studied. For a recent example, see R. Brüning and M. Sutton, Phys. Rev. B **49**, 3124 (1994).

[8] For inorganic glasses the (optical) density has often been determined using the index of refraction; see, e.g., P. B. Macedo and A. Napolitano, J. Res. Natl. Bur. Stand., Sect. A **71A**, 231 (1967).

[9] T. K. Barron, J. G. Collins, and G. K. White, Adv. Phys. **29**, 609 (1980).

[10] See, e.g., C. Meingast, M. Haluska, and H. Kuzmany, J. Non-Cryst. Solids **201**, 167 (1996).

[11] This approach has recently also been used by K. Fukao and Y.

Miyamoto, Europhys. Lett. **46**, 649 (1999); Phys. Rev. E **61**, 1743 (2000).

[12] L. D. Landau and E. M. Lifshitz, *Statistical Physics*, Vol. 5 of *Course of Theoretical Physics* (Pergamon, Oxford, 1980).

[13] J. K. Nielsen and J. C. Dyre, Phys. Rev. B **54**, 15 754 (1996); J. K. Nielsen, Phys. Rev. E **60**, 471 (1999).

[14] If time-reversal symmetry holds, one has $\langle \Delta S(0)\Delta V(t)\rangle = \langle \Delta V(0)\Delta S(t)\rangle$. Thus the order of terms appearing in Eq. (2) may be interchanged.

[15] C. J. F. Böttcher and P. Bordewijk, *Theory of Electric Polarization* (Elsevier, Amsterdam, 1978), Vol. 2.

[16] Here the equilibrium state is to be understood as the metastable melt and of course not the crystalline phase which in most cases will constitute the true equilibrium state close to T_g.

[17] In fact, this expression is equivalent to the Vogel-Fulcher or WLF equation. It involves the fact that the thermal susceptibility is inversely proportional to temperature; see G. W. Scherer, J. Am. Ceram. Soc. **67**, 504 (1984) or Ref. [2].

[18] L. D. Landau and E. M. Lifshitz, *Theory of Elasiticity*, Vol. 7 of *Course of Theoretical Physics* (Pergamon, Oxford, 1986).

[19] For materials with $\nu<0$, see, e.g., R. Lakes, Adv. Mater. **5**, 293 (1993).

[20] In polymeric glasses, ν is rarely smaller than 0.3; see, e.g., W. D. Callister, Jr., *Materials Science and Engineering—An Introduction* (Wiley, New York, 1997).

[21] Other expressions may be used instead, but for the relatively small dielectric constants of interest here, this should make no significant difference.

[22] C. Hansen and R. Richert, Acta Polym. **48**, 484 (1997).

[23] T. Bretz, diploma thesis, Fachhochschule Wiesbaden, 1996.

[24] Taking typical values for K ($\approx$ 1 GPa) and α ($\approx 10^{-4}\,\mathrm{K}^{-1}$), a temperature change of 1 K alters the pressure on the rigid capacitor plates by about 1 bar.

[25] J. A. Forrest, C. Svanberg, K. Révész, M. Rohdal, L. M. Torell, and B. Kasemo, Phys. Rev. E **58**, R1226 (1998).

[26] N. O. Birge and S. R. Nagel, Phys. Rev. Lett. **54**, 2674 (1985); T. Christensen, J. Phys. (Paris) Colloq. **45**, C8-635 (1985).

[27] See, e.g., P. K. Dixon and L. Wu, Rev. Sci. Instrum. **60**, 3329 (1989).

[28] An approximate linearity of response up to oscillation amplitudes of 1–1.5 K was also observed in thermomodulated DSC experiments, J. E. K. Schawe and S. Theobald, J. Non-Cryst. Solids **235-237**, 496 (1998); C. Schick, M. Merzlyakov, and A. Hensel, J. Chem. Phys. **111**, 2695 (1999).

[29] Since in the vicinity of T_g the slope of $C(T)$ is negative, outside of the dispersive range the experimentally determined phase lags are close to 180°.

[30] *Polymer Handbook*, 2nd ed., edited by J. Brandrup and E. H. Immergut (Wiley, New York, 1975).

[31] I. M. Hodge, Macromolecules **20**, 2897 (1987). The alternative set of parameters with $T_2 = 210$ K given in this reference yields somewhat less satisfactory agreement with our data shown in Fig. 9.

[32] For previous comparisons of dilatometric and calorimetric responses, see, e.g., C. T. Moynihan *et al.*, Ann. (N.Y.) Acad. Sci. **279**, 15 (1976); S. Takahara, M. Ishikawa, O. Yamamuro, and T. Matsuo, J. Phys. Chem. B **103**, 792 (1999); **103**, 3288 (1999).

[33] T. Christensen and N. B. Olsen, Phys. Rev. B **49**, 15 396 (1994); J. Non-Cryst. Solids **235-237**, 296 (1998).

[34] C. T. Moynihan, S. N. Crichton, and S. M. Opalka, J. Non-Cryst. Solids **131-133**, 420 (1991).

[35] A. Hensel and C. Schick, J. Non-Cryst. Solids **235-237**, 510 (1998) performed a similar comparison for PS using modulated calorimetry.

[36] D. J. Plazek and K. L. Ngai, Macromolecules **24**, 1222 (1991); R. Böhmer and C. A. Angell, Phys. Rev. B **45**, 10 091 (1992).

[37] R. Böhmer, K. L. Ngai, C. A. Angell, and D. J. Plazek, J. Chem. Phys. **99**, 4201 (1993).

[38] R. Richert and C. A. Angell, J. Chem. Phys. **108**, 9016 (1998).

[39] K. U. Schug, H. E. King, Jr., and R. Böhmer, J. Chem. Phys. **109**, 1472 (1998).

[40] K. Ito, J. L. Green, K. Xu, and C. A. Angell, J. Phys. Chem. **103**, 3991 (1999).

[41] C. Bauer, R. Richert, R. Böhmer, and T. Christensen, J. Non-Cryst. Solids (to be published).

[42] C. T. Moynihan, L. P. Boesch, and N. L. Laberge, Phys. Chem. Glasses **14**, 122 (1973). From their Table 2 we find for the loss-peak amplitude ($\alpha''_{\max}$) normalized by the dispersion step ($\Delta\alpha'$) that $(\alpha''_{\max}/\Delta\alpha') = N = 0.6\beta - 0.1\beta^2$ for $0.3 \leqslant \beta \leqslant 1$.